NREL
NATIONAL RENEWABLE ENERGY LABORATORY

Thermal Study of Inverter Components

Preprint

N. Robert Sorensen, Edward V. Thomas, and Michael A. Quintana
Sandia National Laboratories

Stephen Barkaszi
Florida Solar Energy Center

Andrew Rosenthal
New Mexico State University

Zhen Zhang and Sarah Kurtz
National Renewable Energy Laboratory

Presented at the 2012 IEEE Photovoltaic Specialists Conference
Austin, Texas
June 3–8, 2012

NREL is a national laboratory of the U.S. Department of Energy, Office of Energy Efficiency & Renewable Energy, operated by the Alliance for Sustainable Energy, LLC.

Conference Paper
NREL/CP-5200-55509
June 2012

Contract No. DE-AC36-08GO28308

NOTICE

The submitted manuscript has been offered by an employee of the Alliance for Sustainable Energy, LLC (Alliance), a contractor of the US Government under Contract No. DE-AC36-08GO28308. Accordingly, the US Government and Alliance retain a nonexclusive royalty-free license to publish or reproduce the published form of this contribution, or allow others to do so, for US Government purposes.

This report was prepared as an account of work sponsored by an agency of the United States government. Neither the United States government nor any agency thereof, nor any of their employees, makes any warranty, express or implied, or assumes any legal liability or responsibility for the accuracy, completeness, or usefulness of any information, apparatus, product, or process disclosed, or represents that its use would not infringe privately owned rights. Reference herein to any specific commercial product, process, or service by trade name, trademark, manufacturer, or otherwise does not necessarily constitute or imply its endorsement, recommendation, or favoring by the United States government or any agency thereof. The views and opinions of authors expressed herein do not necessarily state or reflect those of the United States government or any agency thereof.

Available electronically at http://www.osti.gov/bridge

Available for a processing fee to U.S. Department of Energy
and its contractors, in paper, from:

U.S. Department of Energy
Office of Scientific and Technical Information

P.O. Box 62
Oak Ridge, TN 37831-0062
phone: 865.576.8401
fax: 865.576.5728
email: mailto:reports@adonis.osti.gov

Available for sale to the public, in paper, from:

U.S. Department of Commerce
National Technical Information Service
5285 Port Royal Road
Springfield, VA 22161
phone: 800.553.6847
fax: 703.605.6900
email: orders@ntis.fedworld.gov
online ordering: http://www.ntis.gov/help/ordermethods.aspx

Cover Photos: (left to right) PIX 16416, PIX 17423, PIX 16560, PIX 17613, PIX 17436, PIX 17721

Printed on paper containing at least 50% wastepaper, including 10% post consumer waste.

Thermal Study of Inverter Components

N. Robert Sorensen[1], Edward V. Thomas[1], Michael A. Quintana[1], Stephen Barkaszi[2], Andrew Rosenthal[3]
Zhen Zhang[4], and Sarah Kurtz[4]
[1]Sandia National Laboratories, Albuquerque, New Mexico, USA
[2]Florida Solar Energy Center, Cocoa, Florida, USA
[3] New Mexico State University, Las Cruces, New Mexico, USA
[4]National Renewable Energy Laboratory, Golden Colorado, USA

Thermal histories of inverter components were collected from operating inverters from several manufacturers and three locations. The data were analyzed to determine thermal profiles, the dependence on local conditions, and to assess the effect on inverter reliability. Inverter temperatures were shown to increase with the power dissipation of the inverters, follow diurnal and annual cycles, and have a dependence on wind speed. An accumulated damage model was applied to the temperature profiles and an example of using these data to predict reliability was explored.

***Index Terms*—Photovoltaics, Reliability, Temperature**

I. Introduction

Sandia National Laboratories (Sandia) and the National Renewable Energy Laboratory have a long history evaluating the reliability of photovoltaic (PV) systems. Inverters are an integral part of a PV system and must function properly for the system output to be optimized. The lifecycle reliability of power electronic devices is highly dependent on operating temperature, which is related to loads and ambient conditions. Fans and heat sinks are employed to mitigate heating of components in an attempt to improve long-term reliability. There are many existing publications focusing on temperature assessment of PV modules and solar heat collectors [1-4], but fewer references discussing the temperature and reliability evaluation for the PV inverter and related components. Knowledge of the thermal history of individual components (capacitors, IGBTs, transformers, circuit boards, heat sinks, etc.) may be useful in assessing system reliability.

This paper includes three primary parts: documentation of measured inverter temperatures, analysis of this data, and the application of these to reliability modeling.

II. Temperature Measurement

Inverters may operate at a wide range of temperatures. A comprehensive model for predicting the temperatures as a function of conditions for all types of inverters is beyond the scope of this paper, but we take an initial step in that direction by developing a model to predict the inverter heat sink temperature as a function of open-rack conditions based on observed heat-sink temperatures. This model must be extended to be able to predict component temperature data; for the reliability calculations we use temperatures measured directly for the components of interest.

The inverter heat-sink temperatures were measured for inverters connected to three grid-connected PV test systems in Golden, Colorado, US. The inverters were installed in the open under each latitude-tilted PV array, and the temperature sensors were fixed in the heat sink of each inverter.

To verify a model of inverter temperature rise[5] and calculate wind speed factor and heat sink factor of the inverter, more than one year of inverter DC /AC power, irradiance, wind speed, and heat sink temperature rise data (5 min averaged per data point) were collected.

For the collection of the inverter component temperature history, six inverters (three manufacturers with similar inverters going into both locations) located in Florida and New Mexico were instrumented with thermocouples to monitor the temperature of individual inverter components. Four-channel data loggers were used to record the temperature of three components and the internal ambient for each of the inverters. Data were collected at 30 second intervals, and then filtered to provide 10 minute measurements. The data were downloaded from the data loggers on a monthly basis for analysis.

An example of thermocouple placement is shown in Figure 1. In this image two thermocouples are visible. One is attached directly to the side of one of the large filter capacitors. The second is used to measure the ambient temperature in the inverter.

For the component study, specific components in six inverters were instrumented (2 inverters in the New Mexico, 4 in the Florida). The locations for the thermocouples for each of the inverters were:

- Inverter FA1 – Upper cabinet ambient, capacitor, control board, transformer
- Inverter FB1 – Capacitor, control board, coil, transformer
- Inverter FC1 – Capacitor, control board, small capacitor / torroid, relay
- Inverter FC2 – TC1. Heat sink, capacitor, internal ambient
- Inverter SB1 – Torroid, heat sink, capacitor, fuse
- Inverter SD1 – Transformer, capacitor, inverter backplane, ambient

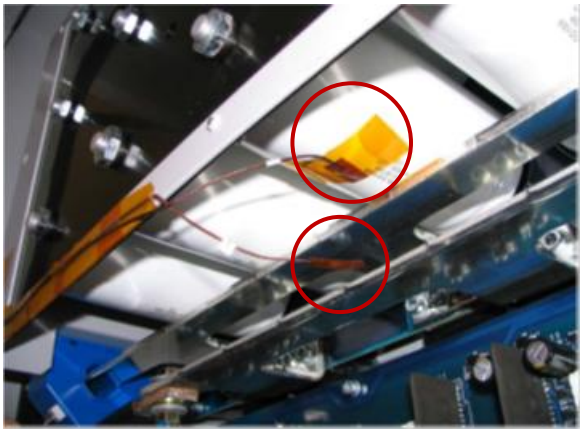

Figure 1. Photograph showing placement of thermocouples on inverter components

III. Inverter Temperature Calculations

We expect that the temperatures of components in inverters may be modeled by understanding 1) a function defining the difference between the ambient temperature and heat-sink temperature and 2) the dissipation of heat in each component and the associated temperature drop between the component and the heat sink. The first of these we expect to be dependent on the total heat dissipation, the transfer (both convective and radiative) of heat from the heat sink depending on the area of the heat sink and other aspects of the heat sink design, and the wind speed, which provides forced cooling. We propose to model the difference between the ambient and heat sink temperatures, ΔT, as

$$\Delta T = \frac{k}{(1+c\times Vw)} \times \frac{(Pdc-Pac)}{Pr} \quad (1)$$

where *Pdc, Pac, Pr, Vw, c* and *k* represent the input DC power, the output AC power, the rating power of the inverter, the wind speed, the wind speed factor and heat sink factor of the inverter, respectively.

The temperature difference between the inverter components and the heat sink can be approximated by:

$$\Delta T' = k' \times Pc \quad (2)$$

where $\Delta T'$ is the temperature difference between each inverter component and heat sink, *Pc* is the consumed power of the inverter components and *k'* is the heat transfer coefficient of each inverter component. Each inverter components' temperature, *Tc*, can be calculated from eqs 1 and 2 by:

$$Tc = Ta + \Delta T + \Delta T' \quad (3)$$

where *Ta* is the ambient temperature. In general, each component may have a different level of heat dissipation and thermal connection, so equation 3 may be written for each component.

Equation 1 was used to fit the heat sink data measured for one of the three inverters installed in Colorado. For this inverter, k was found to be 387 (°C) and c to be 0.29 (s/m). Similar analysis for other inverters found k to range from 350 to 650 (°C) and c from 0.20 to 0.30 (s/m). Figure 2 shows how instantaneous measurements of the inverter temperature are correlated with the model (R^2 = 0.71). The fit is much better when the data are averaged (R^2 = 0.98). In this case, the average temperature points were obtained by averaging 50 different temperature values for the inverter with the same inverter consumed power ratio and equivalent wind speed. For the purpose of evaluating reliability of inverters, knowledge of the average temperature may be adequate, alleviating the need to develop a transient model, though degradation processes that have high activation energies may be dominated by the short times spent at high temperatures.

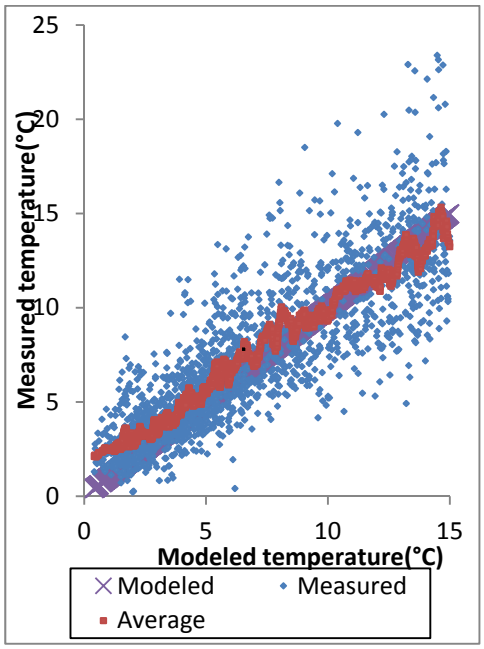

Figure 2. Comparison between the temperatures that were measured and modeled using eq. 1. The blue data reflects individual data points; the red data shows the average of 50 temperature values for the same modeled temperature.

IV. General Observations

Data from the six inverters in Florida and New Mexico were analyzed to provide insight into thermal management issues in general and for specific inverter/location combinations. Figure 3 presents data for inverter SB1. Several observations can be made from the data. There is a significant daily swing in temperature that can be seen for all of the components. Additionally, the temperature varies among individual components. In this case the torroid operated at a significantly higher temperature than did the fuse. A seasonal variation can also be seen. The temperature range (max to min) does not appear to be season-dependent, but the mean temperature correlates with the time of the year (hotter in the summer, colder in the winter).

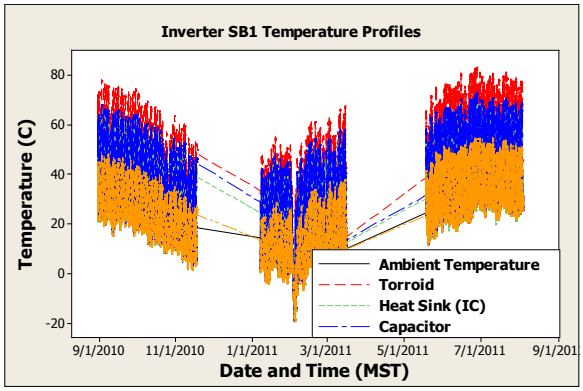

Figure 3. Temperature profile for inverter SB1. Gaps in data correspond with datalogger malfunction.

An attempt was made to simplify data collection and manipulation by determining the average daily temperature. Doing so captures any seasonal variability, but completely misses the diurnal swings (see Figure 4). Thus, while daily mean temperatures may be useful in comparing components, it is not sufficient to assess the effect of temperature on component reliability.

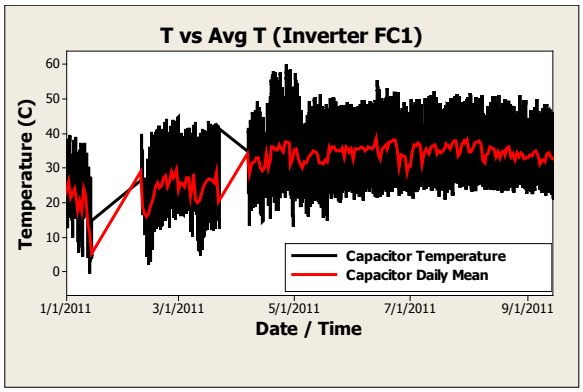

(a)

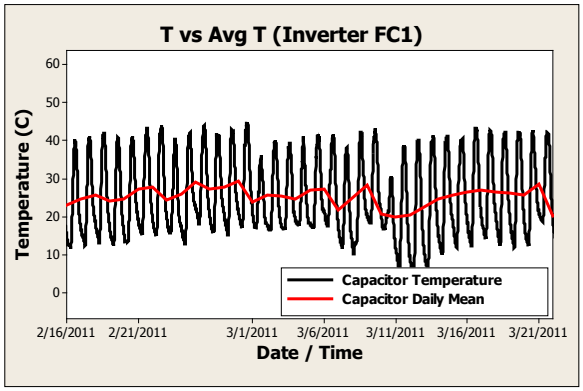

(b)

Figure 4. Plots showing average daily temperature and 10-minute measurements. The figure in (a) is for several months while the plot in (b) represents about 1 month.

Figure 5 shows temperature profiles for inverter FA1 during the month of July. The components included in this data set are a capacitor, the IGBT control board, and the transformer. In addition, a thermocouple recorded the temperature in the enclosure (Upper Ambient). An internal reference in the data logger also recorded the ambient temperature. As seen in Figure 5, the highest temperatures were recorded for the IGBT control board and the transformer. The maximum temperature recorded was around 60°C. The diurnal nature of the temperature profile is obvious. Components heat up during the day and cool down at night. However, it is interesting to note that, while the temperature of the capacitor and transformer approached ambient at night, the IGBT control board did not. This poses a question about how inverter parasitic power should be described in performance specifications.

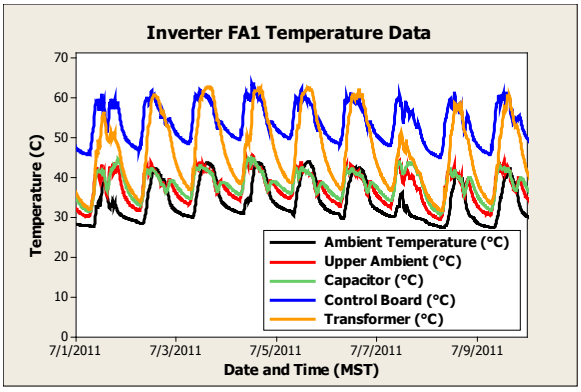

Figure 5. Temperature profiles obtained during the month of July from inverter FA1. The three instrumented components included the capacitor, IGBT control board, and transformer.

It is useful to consider the empirical cumulative distribution function (ECDF) of the temperature data (see Figure 6). The ECDF enables the entire temperature profile to be easily evaluated. In Figure 6, ECDFs are displayed for both January and July (separately), as well as the total time period. The solid curve represents overall results. The dashed lines are for the individual months. From these plots, a definite seasonal influence can be seen. As expected, there is a significant shift of the ECDF to higher temperatures for the month of July.

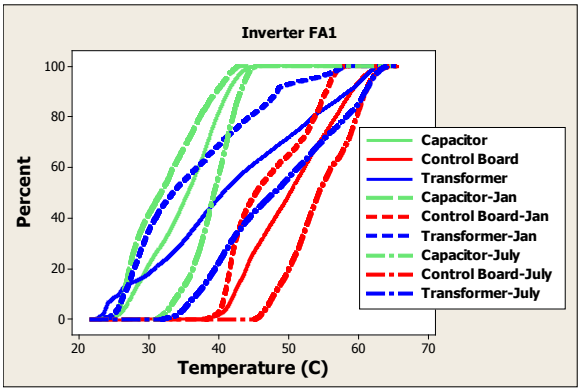

Figure 6. ECDF profiles for the three instrumented components during the months of January and July. The dashed curves represent measurements taken in January.

Figure 7 presents temperature distributions for the three components and the ambient from inverter FA1 for the month of January. Consistent with the temperature profiles, the IGBT

control board shows no history of low temperatures, indicating that it remains warm, even during periods of non-operation. In contrast, the transformer and capacitor temperatures include the range for the ambient temperature. Note that the transformer and IGBT control board exhibit temperatures considerably higher than either the ambient or the capacitor.

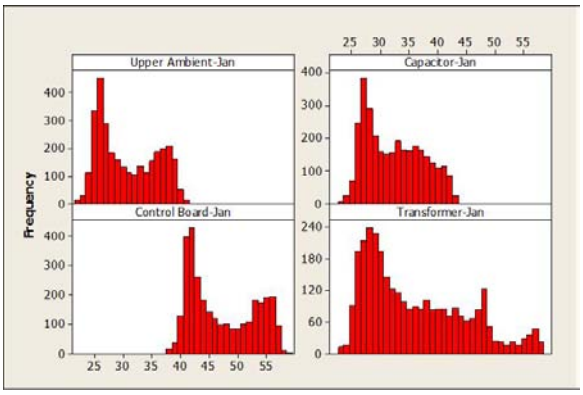

Figure 7. Thermal profile (distribution) for the month of January.

Figure 8 summarizes the thermal data for inverter FA1. The side-by-side boxplots indicate the distribution of temperature for each of the components. Separate summaries are included for the whole period of record (January through July), as well as for January and July, separately. From these data it is easy to see the seasonal effect on each of the components. From this plot, it is clear that the control board was exposed to the highest temperature followed by the transformer and the capacitor. The capacitor temperature was essentially the same as the ambient inside the inverter. For the control board, the temperature difference between winter and summer was about 10°C.

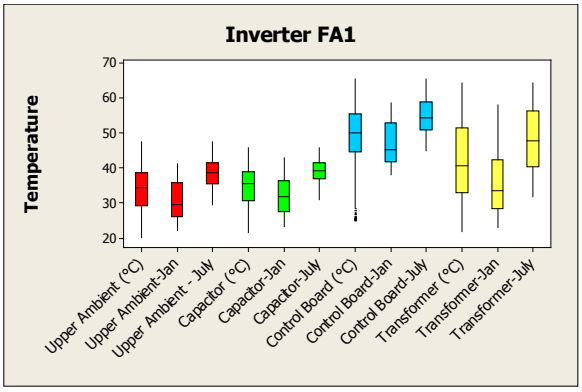

Figure 8. Boxplot of temperatures for inverter FA1 showing the difference in temperature associated with season.

One of the monitored inverters (SD1) exhibited temperatures in excess of 100ºC for the transformer, as shown in Figure 9. It is clear from the ECDF (Figure 9b) that the transformer was hotter than the rest of the inverter, and the overall temperature was higher than for other inverters in this study.

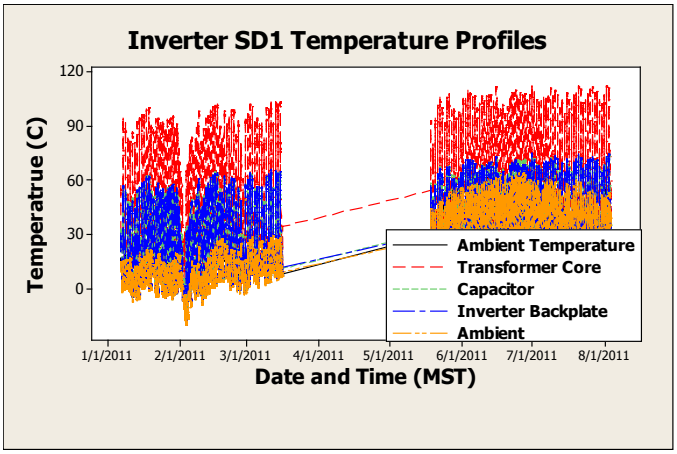

(a)

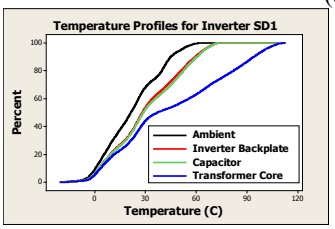

(b)

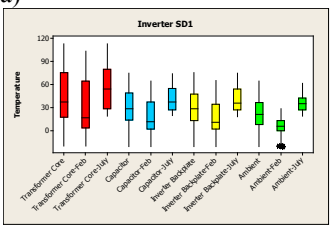

(c)

Figure 9. Thermal history for inverter SD1. Missing data are the result of data logger issues. Plots shown in (b) and (c) depict complete thermal history.

Based on a simple evaluation of temperature for the two sets of inverters in this study, several conclusions can be drawn:

1. As would be expected, the external ambient has an effect on inverter temperature. The overall temperature is higher in the summer and lower in the winter.
2. The range of temperature (daily swing) that appears to be due to operational heating (on *vs*. off) is larger than the change in temperature due to seasonal changes.
3. Significant temperature differences were observed among the inverters resulting from both design differences and location dependencies.
4. Monitoring the daily mean temperature (for individual components or for the inverter ambient) does not capture the extreme differences in inverter or component temperature.
5. The temperature of individual components can vary significantly. Simply monitoring the internal ambient does not provide sufficient information to draw accurate conclusions about reliability of components.
6. Modeling of the temperature will be a function of inverter design, deployment geometry and weather conditions and will require substantially more study to be able to understand the full picture.

I. Accumulated Damage Model

In addition to making general observations for inverter components, the data collected can be used in an assessment of inverter and/or component reliability. If we assume a thermally-activated degradation mechanism, we would like to know the failure-time distribution for the components over a varying temperature profile. In order to do that, information

about the activation energy must be known. To demonstrate the process, we can assume that the activation energy has been estimated experimentally via a series of accelerated aging tests over a range of temperatures. We can then use a cumulative exposure model with the temperature data taken from the inverters to evaluate the failure-time distribution.

The cumulative exposure model assumes that an increment of degradation occurs during each increment of time, and depends on the temperature during that time increment[7].

First, to digress, assume a fixed exposure at temperature (T). The failure-time distribution function is an exponential containing the degradation rate at time (t), given by:

$$F(t;T) = 1 - \exp[-\lambda(T) \times t] \tag{4}$$

where λ is the incremental degradation rate. That is, *F(t;T)* is the fraction of units that have failed by time (*t*) The degradation rate is a function of temperature given by:

$$\lambda(T) = A \times \exp\left[\frac{-E_a / R}{T}\right] \tag{5}$$

where E_a is the activation energy and R is the universal gas constant[7].

Now consider a variable temperature exposure, where $\Delta_{T(i)}$ and $\lambda_{T(i)}$ represent the time and degradation rate at temperature $T(i)$ for $i = 1,2,\cdots,n$. The degradation rate during each time interval depends on $T(i)$ through the Arrhenius equation[2]. Assuming the cumulative exposure model, the fraction of units that have failed after such an exposure is $F = 1 - exp[-\varepsilon]$, where

$$\varepsilon = \Delta_{T(1)} \times \lambda_{T(1)} + \Delta_{T(2)} \times \lambda_{T(2)} + \ldots + \Delta_{T(n)} \times \lambda_{T(n)} \tag{6}$$

The effective degradation rate for such an exposure is given by

$$\lambda_{eff} = \frac{\varepsilon}{\sum_{i=1}^{n} \Delta_{T(i)}} \tag{7}$$

We can use the above equations to predict a hypothetical failure probability for an inverter. Assume that mean time to failure (MTTF) is 5000 hours at 55ºC. For an exponential model, MTTF = 1/λ. Thus, λ(T) is 0.0002 at 328K. Assume that E_a/R is 6000K (it might vary from 3000K to 12,000K). Plugging those values into the equation 5 gives:

$$0.0002 = A \cdot exp(-6000/328) \tag{8}$$

which provides a value of $1.76X10^4$ for the pre-exponential, A.

Figure 10 shows the temperature ECDF for an inverter with data collected over an extended time period. The data set contains 2481 intervals of 10 minutes each. We can assume that the ECDF is representative of the distribution of temperature throughout the whole year. The effective degradation rate (λ_{eff}) based on the ECDF can be used to estimate the failure probability versus time via

$$F(t) = 1 - exp[-\lambda_{eff} \cdot t] \tag{9}$$

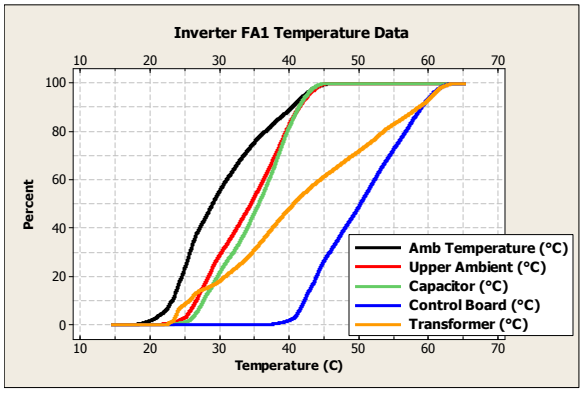

Figure 10. Empirical CDF curves for components instrumented with thermocouples.

Figure 11 shows the predicted probability of failure for the transformer, IGBT control board and capacitor for inverter FB1. These curves are based on the assumption of 5000 hours for a mean time to failure, and an activation energy (E_a/R) of 6000K. In this case, the control board, which had the highest cumulative temperature, is the most likely component to fail, followed by the transformer and the capacitor.

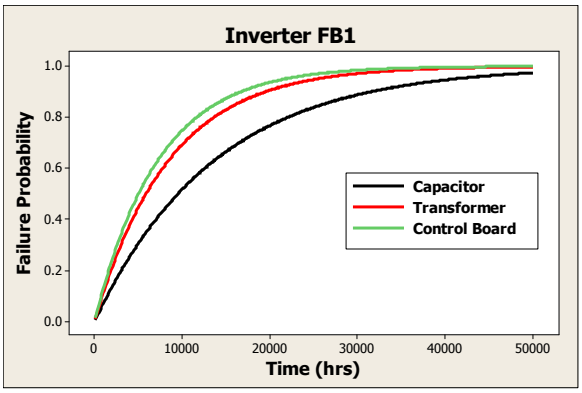

Figure 11. Failure probability curves using an activation energy (E_a/R) of 6000K, and a MTTF value of 5000 hours for these three components.

We can evaluate other failure mechanisms by allowing individual components to have unique values of MTTF and/or activation energy. Figure 12 and Figure 13 show how the failure probability curves vary for alternate values of MTTF for the three components. As seen in Figure 13, lowering the MTTF for capacitors to 2000 hours results in the capacitor becoming the life-limiting component. These techniques can be used to perform trade-off studies in assessing system reliability. They also suggest that accelerated testing of individual components to obtain activation energies can be used to generate higher fidelity reliability predictions.

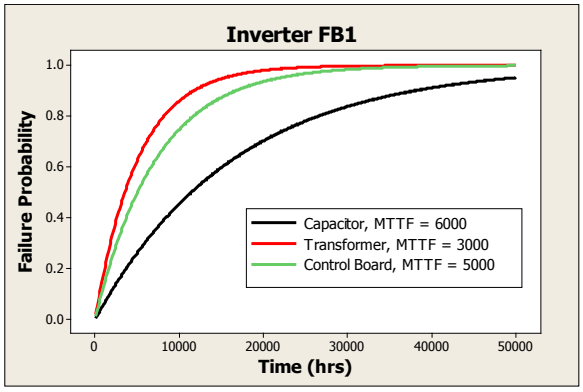

Figure 12. Failure probability curves using an activation energy (E_a/R) of 6000K, and MTTF values of 5000, 3000, and 6000 hr for the transformer, IGBT control board and capacitor, respectively.

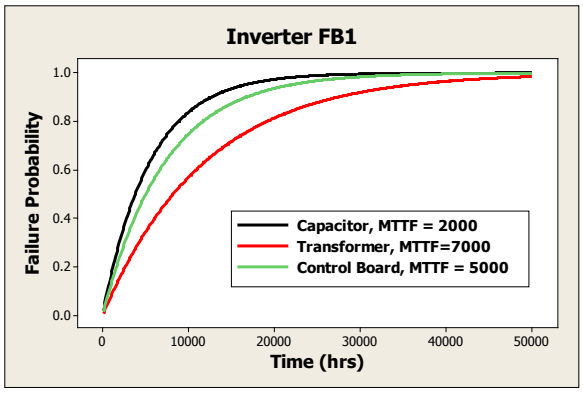

Figure 13. Failure probability curves using an activation energy (E_a/R) of 6000K, and changing the MTTF value for the IGBT control board.

We can use this process to compare components of various inverters. Figure 14 shows the predicted reliability of the six inverters based only on capacitor thermal data. It is assumed that all of the capacitors have the same MTTF (5000 hrs at 55ºC) and the same activation energy (E_a/R = 6000K). As can be seen in this plot, there is some correlation with location. The two inverters exhibiting the highest predicted reliability (FC1 and FA1) are both located in the southeast. The other group of 4 inverters includes FC2, FB1 (both in the southeast) and SB1 and SD1 (located in the southwest. From these data, it appears that the type of inverter and possible installation details (location, solar exposure, indoors, outdoors, shading, etc.) are more important than geographical location, although location does appear to play a role. An examination of the CDF plots for each system (Figure 14 b) shows an obvious correlation between CDF and reliability for the two inverters located in the southwest (SB1 and SD1), but the link between CDF and reliability is less obvious for the other four inverters. Of particular interest is the profile for FA1. The CDF is steep suggesting a smaller range of temperatures for this component. It gets neither hot nor as cold as the other inverters, but the mean temperature is higher.

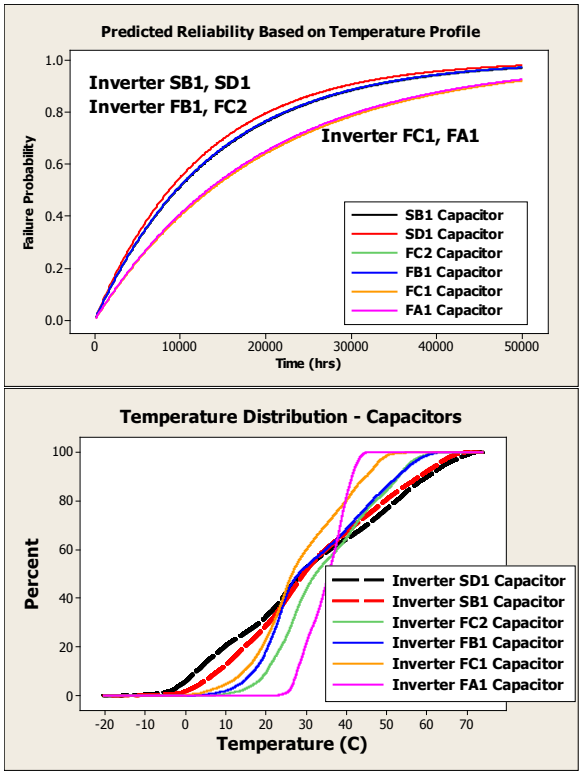

Figure 14. Calculated reliability of capacitors based on thermal profile using the accumulated damage model. For this example, the MTTF was assumed to be 5000 hours with an activation energy (Ea/R) of 6000K

A similar evaluation can be made for control board reliability. In this case, the three inverters were all located in the southeastern US. Figure 15 shows predicted reliability based on the control board thermal data for inverters FB1, FA1, and FC1. In this case, the control board for inverter FC1 exhibited the highest predicted reliability (assuming identical MTTF and E_a values). The CDF temperature plots (shown in (b)) show the correlation between temperature and reliability. The control board in FC1 has the lowest overall temperature. The other two (FA1 and FB1) exhibit almost identical reliability curves, but their thermal profiles differ considerably. The inset in (b) shows the histogram for FB1, which is a bimodal distribution. In this case, the control board cools down substantially during the night and heats up during the day.

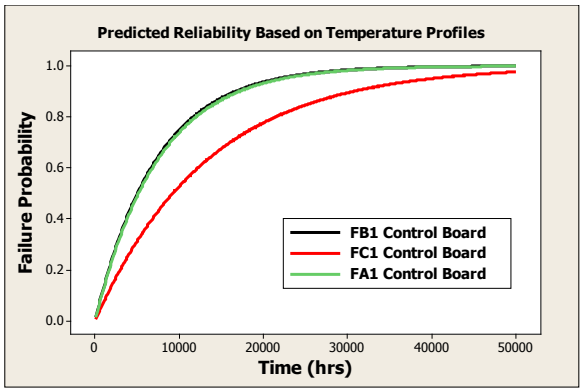

(a)

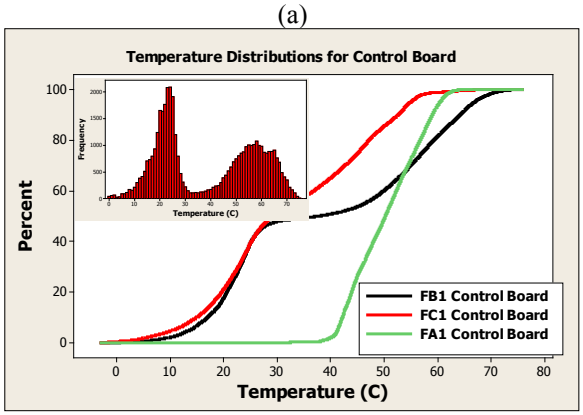

(b)

Figure 15. Comparison of reliability calculations for control boards in inverters FB1, FC1, and FA1 (all located in the Southeast). The reliability plots are shown in (a) with the corresponding temperature profiles in (b) and temperature histogram (inset). Reliability calculations are based on MTTF of 5000 hrs and an activation energy (E_a/R of 6000).

The above demonstrations are based on knowing both mean time to failure and activation energy. To predict actual reliability of an inverter, estimates of MTTF and E_a are required. They will need to be obtained through accelerated test data over a range of temperatures.

This process of predicting reliability based on an accumulated damage model can be a useful tool for analyzing and improving inverter and PV system reliability. In this example, the stress being considered was temperature. This type of analysis is not limited to thermal stress. The same techniques can be used for other stresses such as mechanical or electrical. Once the stress profiles are collected, and given a relationship between the particular stress and a degradation mechanism, the accumulated damage process can be used to predict reliability.

II. Summary

We have demonstrated how temperature profiles from inverter components can be analyzed to provide insight into inverter reliability. They can be used without extensive analyses to compare inverters, inverter components, and installations details. By assuming values of mean time to failure and activation energies for the individual components, the results can be used to predict reliability (probability of failure).

A detailed understanding of inverter temperature will require more study, but the thermal history data elucidated how the inverter temperatures are dependent on the ambient conditions even when the inverters are enclosed, how parasitic power can affect the temperature of individual components, and how the effects of wind and ambient temperature can be modeled to understand the inverter heat sink temperature.

Acknowledgment

Sandia National Laboratories is a multi-program laboratory managed and operated by Sandia Corporation, a wholly owned subsidiary of Lockheed Martin Corporation, for the U.S. Department of Energy's National Nuclear Security Administration under contract DE-AC04-94AL85000.

This work was supported by the U.S. Department of Energy under Contract No. DE-AC36-08-GO28308 with the National Renewable Energy Laboratory.

References

[1] Aljoaba, S.Z., A.M. Cramer, and B.L. Walcott. Thermo-electrical modeling of light wavelength effects on photovoltaic cell performance. in Photovoltaic Specialists Conference (PVSC), 2011 37th IEEE. 2011.

[2] Bharti, R., J. Kuitche, and M.G. TamizhMani. Nominal Operating Cell Temperature (NOCT): Effects of module size, loading and solar spectrum. in Photovoltaic Specialists Conference (PVSC), 2009 34th IEEE. 2009.

[3] Cotal, H. and J. Frost. Heat transfer modeling of concentrator multijunction solar cell assemblies using finite difference techniques. in Photovoltaic Specialists Conference (PVSC), 2010 35th IEEE. 2010.

[4] Kumar, S. and S.C. Mullick, Wind heat transfer coefficient in solar collectors in outdoor conditions. Solar Energy, 2010. 84(6): p. 956-963.

[5] Zhang, Z., Sorensen, R., and Kurtz, S. Heat Transfer Study on Open-Rack Installed Photovoltaic Inverters, to be published.

[6] Wayne Nelson, Accelerated Testing: statistical models, test plans and data analysis, Wiley-Interscience, 2004.